Heat Recovery Systems & CHP Vol. 10, No. 2, pp. 161–175, 1990
Printed in Great Britain

0890-4332/90 $3.00 + .00

AN EVALUATION OF A RANKINE CYCLE DRIVEN HEAT PUMP

R. N. CHRISTENSEN
The Ohio State University, Mechanical/Nuclear Engineering, 206 W. 18th Ave Columbus, OH 43210, U.S.A.

M. SANTOSO
Mechanical Engineering, The Ohio State University Columbus, OH 43210, U.S.A.

(*Received* 6 *July* 1989)

Abstract—This paper discusses a configuration of a Rankine cycle engine-driven heat pump, and includes a theoretical investigation of its performance characteristics. The system employs a Rankine power cycle, using R-113 as the working fluid, coupled to a vapour compression cycle heat pump using R-22. A novel feature of the concept is the use of hydraulically connected rolling diaphragm piston-cylinder devices as motor, compressor and pump.

Heating and cooling *COP*s of 2.01 and 1.06 respectively are predicted, making the system potentially attractive where both heating and cooling are required.

INTRODUCTION

Today's electric heat pump system uses a vapor compression cycle. The refrigerant removes heat from the environment in the evaporator. It is compressed in an electrically driven compressor, and then sent to a condenser. The condenser rejects heat to the heat sink, and then the refrigerant flows back to the evaporator through an expansion valve.

The most significant energy consumer of this cycle is the electric motor driving the compressor. With respect to the electrical energy utilized by the cycle, the system has a moderate (1.1–2.5) system coefficient of performance in both the heating and the cooling modes. However, due to the low electrical generation efficiency, the electrtic heat pump *COP* with respect to the original energy source (natural gas or oil) is much lower.

The typical efficiency of an electric power plant is about 32%, and approximately 3% of the electricity is lost during transmission process, leaving only 29% of the energy supplied by the fuel to be utilized as electrical energy. Consequently, the actual *COP* value of the electric heat pump system is less than a third of the value obtained with respect to the compressor work.

In an effort to improve *COP*, some of the alternative cycles that utilize the energy source directly (oil or natural gas) are the Brayton or Rankine cycle engine-driven heat pumps. The power cycle in this system generates energy to drive the compressor for the vapor compression cycle. Friedman [1], proposed a space conditioning system which employs a Brayton cycle engine as the power generator. Other researchers, Swenson and Rose [2], developed a high seasonal performance factor gas heat pump using a Rankine cycle engine as the power generator.

It is felt, however, that those two systems do not exhibit an acceptable *COP* in both heating and cooling. Consequently, in this study an alternative configuration of a Rankine cycle engine-driven heat pump system is proposed, and its performance characteristics are investigated.

ALTERNATIVE CONFIGURATION OF A RANKINE CYCLE ENGINE-DRIVEN HEAT PUMP SYSTEM

The proposed system is given in Fig. 1. It consists of a Rankine power cycle and a vapor compression cycle. The Rankine cycle utilizes R-113 as its refrigerant fluid, while the vapor compression cycle uses R-22. The motor, compressor, and pump used in this system are patented rolling diaphragm piston-cylinder devices that are interconnected hydraulically. Three heat exchangers are added to the system to increase *COP*. They are the refrigerant heat exchanger, a recuperative heat exchanger, and a triple tube heat exchanger.

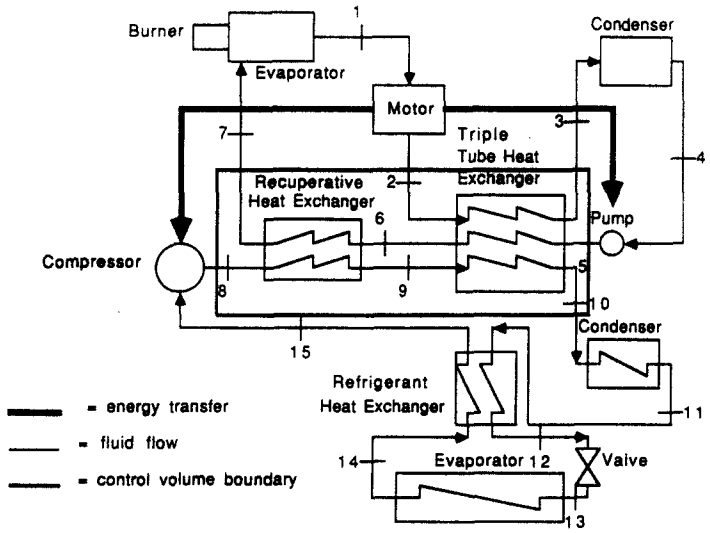

Fig. 1. The configuration of the new cycle.

In the vapor compression part of the cycle, the R-22 in the evaporator removes energy from the environment. The refrigerant is then compressed and sent to the condenser to deliver heat to the heat sink. From the condenser, the R-22 is delivered back to the evaporator through an expansion valve. In the Rankine cycle, the R-113 inside the evaporator receives energy from a natural gas burner. The R-113 is heated to a saturated vapor, and is used to drive the positive displacement motor. From the motor, the R-113 is sent to the condenser via the triple tube heat exchanger. The R-113 leaves the condenser in a saturated or sub-cooled condition, and then is pumped back to the evaporator.

During the cycle, the R-113 and R-22 pass through the refrigerant, recuperative, and triple tube heat exchangers. The refrigerant heat exchanger transfers energy from the R-22 leaving the condenser to the R-22 going to the compressor. The purpose of the recuperative heat exchanger is to use the R-22 leaving the compressor to preheat the R-113 going to the evaporator.

The triple tube heat exchanger also preheats the R-113 solution going from the pump to the evaporator. Referring to Fig. 1, heat is transferred from both the R-113 between state 2 and 3, and from the R-22 between state 9 and 5 to the R-113 between state 5 and 6. The objective of these three heat exchangers is to minimize the energy required to heat the R-113 to a saturated vapor state.

As indicated in Fig. 1, the power generated by the hydraulic motor is used to drive the pump and the compressor. Some energy is lost during this process due to mechanical inefficiency. In this case, the mechanical efficiency is defined as the ratio of the power received by the pump and the compressor to the power produced by the hydraulic motor. This efficiency can be formulated as:

$$\eta_{\text{mech}} = \frac{m_{22}(h_8 - h_{15}) + m_{113}(h_5 - h_4)}{m_{113}(h_1 - h_2)} \tag{1}$$

where m_n = mass flow rate of refrigerant n and h_n = enthalpy at state n.

ANALYSIS OF THE PROPOSED CYCLE

In the cycle analysis, a control volume is drawn around the recuperative and triple tube heat exchangers, making one heat exchanger (Fig. 1) and simplifying the calculations. Depending on manufacturing constraints, the function of these two components may be accomplished by a single triple tube heat exchanger. This could reduce the cost of the system development by eliminating an unnecessary component.

The system *COP*, the condenser *UA*s and the evaporator *UA* are the quantities of interest in this study. The derivation of the *COP* equation starts with the conservation of energy principle around the control volume. Referring to Fig. 1, the equation is:

$$m_{113}\eta_{\text{mech}}(h_1 - h_2) = m_{22}(h_8 - h_{15}) + m_{113}(h_5 - h_4). \tag{2}$$

Manipulation of the above equation yields the following mass flow rate ratio equation:

$$\frac{m_{22}}{m_{113}} = \frac{h_4 - h_5 + (h_1 - h_2)\eta_{\text{mech}}}{h_8 - h_{15}}. \tag{3}$$

In the cooling mode, the system *COP* is defined as the ratio of the energy removed from the heat source to the energy supplied to the R-113 evaporator. The *COP* is therefore defined as

$$COP = \frac{m_{22}(h_{14} - h_{13})}{m_{113}(h_1 - h_7)}. \tag{4}$$

Substituting equation (3) for m_{22}/m_{113}, yields:

$$COP = \frac{h_4 - h_5 + (h_1 - h_2)\eta_{\text{mech}}}{h_8 - h_{15}} \times \frac{h_{14} - h_{13}}{h_1 - h_7}. \tag{5}$$

In the heating mode, the *COP* is defined as the ratio of the energy released by the condenser to the heated space to the energy supplied to the R-113 evaporator:

$$COP = \frac{m_{22}(h_{10} - h_{11}) + m_{113}(h_3 - h_4)}{m_{113}(h_1 - h_7)}. \tag{6}$$

Again substituting equation (3) for m_{22}/m_{113} gives:

$$COP = \left(\frac{h_4 - h_5 + (h_1 - h_2)\eta_{\text{mech}}}{h_8 - h_{15}} \times \frac{h_{10} - h_{11}}{h_1 - h_7}\right) + \frac{h_3 - h_4}{h_1 - h_7}. \tag{7}$$

In order to find the *UA* of the condensers and the R-22 evaporator, a heat balance is taken on each component, and the heat transferred is related to the change in temperature of the air passing through the component.

For the R-22 evaporator, those equations are:

$$Q = m_{22}(h_{14} - h_{13}), \tag{8}$$

$$Q = m_a C_p (T_{ai} - T_{ao}) \tag{9}$$

and

$$Q = UA\Delta T_{lm}. \tag{10}$$

Combining equation (8) and (9) and solving for the air outlet temperature gives:

$$T_{ao} = T_{ai} - \frac{m_{22}(h_{14} - h_{13})}{m_a C_p}. \tag{11}$$

For the R-22 evaporator, equation (11) is then included in the definition of log-mean temperature difference as:

$$\Delta T_{lm} = \frac{T_{ai} - T_{ao} - T_{14} + T_{13}}{\ln\left[\dfrac{T_{ai} - T_{14}}{T_{ao} - T_{13}}\right]}. \tag{12}$$

Combining equations (8) and (10) results in:

$$UA = \frac{m_{22}(h_{14} - h_{13})}{\Delta T_{lm}}. \tag{13}$$

where

T_{ai} = air temperature entering the evaporator,
T_{ao} = air temperature leaving the evaporator,

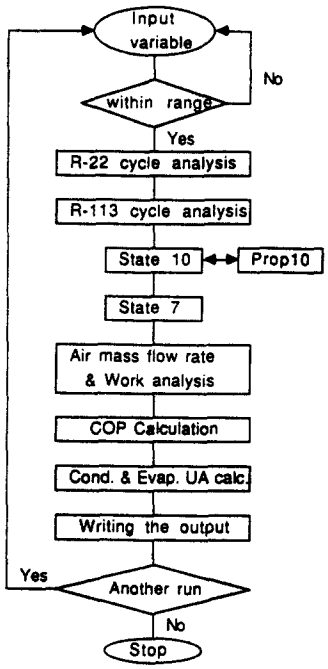

Fig. 2. Main flow chart of the computer program.

C_p = air heat transfer coefficient,
m_a = air mass flow rate,
Q = amount of heat transfer between air and refrigerant.

For the R-22 and R-113 condensers, the same derivation is used to obtain UA.

In order to investigate the COP behavior, a parametric analysis of this cycle was conducted. This analysis involved varying several operating variables. The objective was to relate system operating conditions to COP and component size, and to investigate component effectiveness in enhancing COP. To achieve this goal, a computer program which calculated COP and component UAs as a function of system operating conditions was written.

For given operating conditions, the program finds all necessary state properties and performs calculations to find COP and UA of the heat exchangers using the equations given above. The program logic is given in Fig. 2. At the beginning of the program, the user specifies the operating conditions in an interactive manner. During this process, the program checks the values entered to determine if they are within the property range that the program can handle. If not, the program will stop the execution and prompt an error message.

Once the process of entering operating conditions is complete, the calculation process finds the properties at all of the necessary states in the R-22 cycle and then the properties in the R-113 cycle. Next, the COP and the heat exchangers' UA are calculated. The program will then ask the user if another case is to be run.

RESULTS OF COOLING MODE PARAMETRIC ANALYSIS

In the cooling mode, the parametric analysis was performed by varying the following parameters:

(1) R-113 evaporator operating pressure;
(2) the hydraulic motor and compressor isentropic efficiency;
(3) R-22 and R-113 condenser operating temperatures;
(4) outdoor or environmental temperature;
(5) system mechanical efficiency;
(6) R-22 evaporator operating temperature;
(7) refrigerant heat exchanger effectiveness;
(8) triple tube heat exchanger effectiveness.

Table 1. Base parameters of cycle for heating and cooling modes

Parameter	Cooling	Heating (45°F)	Heating (17°F)
Heat sink (outdoor air) temperature	95°F	68°F	68°F
Heat source (indoor air) temperature	78°F	45°F	17°F
Mechanical efficiency (defined in equation (1))	0.9	0.9	0.9
System cooling capacity	3 ton	3 ton	3 ton
Triple tube heat exchanger cooling effectiveness	0.9	0.9	0.9
R-22 evaporator operating temperature	35°F	9°F	−19°F
R-22 condenser operating temperature	124.1°F	110°F	110°F
R-113 condenser operating temperature	137.8°F	119°F	127°F
Motor and compressor isentropic efficiency	1.0	1.0	1.0
Air flow rate through R-22 evaporator	1700 cfm	2000 cfm	2000 cfm
Air flow rate through R-22 condenser	2000 cfm	790 cfm	800 cfm
Air flow rate through R-113 condenser	2000 cfm	910 cfm	1070 cfm
All subcooled and superheated temperature differences	2°F	2°F	

While each of these parameters is varied, the other operating conditions are fixed in order to find the *COP* variation with respect to that particular variable. In the cooling mode, the rated operating condition is an outdoor temperature of 95°F. See Table 1 for a listing of the base parameters for each operation mode.

The results of the parametric analysis of variables 1–8 above are presented in Figs 3–13. In some of these figures, the R-22 evaporator and R-22 and R-113 condensers' *UA* variation with respect to the independent variables are included; however, the *COP* behavior is still the main objective of this analysis. The purpose of including the *UA* values is to determine the heat exchanger size required to achieve the *COP* attained by these specific operating conditions. The reverse is not true, however. Given a specific heat exchanger size, the system performance under other operating conditions cannot be determined from the figures presented here. To find system performance, the user would need to perform a trial and error procedure, varying superheated and/or subcooled temperature differences using the computer code. The code is, therefore, a design tool and not a system performance tool.

Referring to Fig. 3, it is observed that the system *COP* increases as the R-113 evaporator operating pressure is increased. This pressure increase corresponds to a higher R-113 evaporator temperature. Consequently, it is more beneficial to operate the system at the highest R-113 evaporator operating pressure possible. In the figure, two *COP* values are given. These two values correspond to *COP* values when the system mechanical efficiency is 100% and 90%, respectively.

In Fig. 4, the *COP* is observed to increase as the isentropic efficiency is increased. In this analysis, the hydraulic motor and compressor efficiencies are assumed to be the same to simplify the calculation and analysis involved. Experiments with a prototype compressor at The Ohio State University have shown that the motor/compressor unit exhibits an isentropic efficiency of nearly 98% and a mechanical efficiency of 90%. The equation relating *COP* to isentropic efficiency can

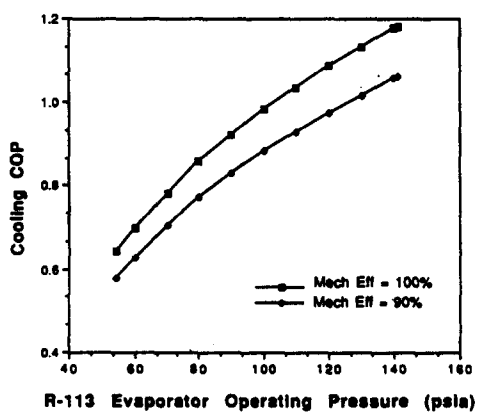

Fig. 3. Cooling *COP* vs R-113 evaporator operating pressure.

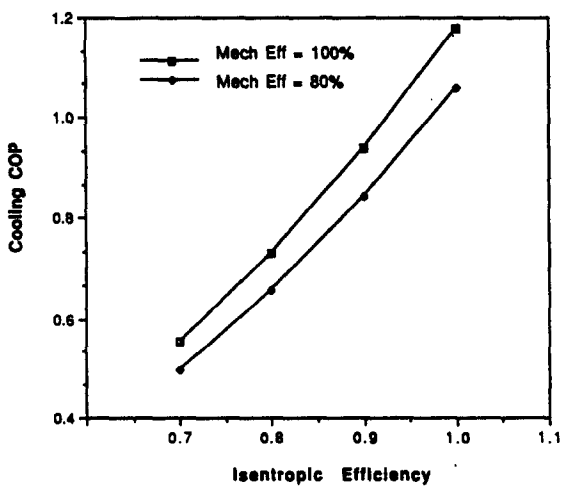

Fig. 4. Cooling *COP* vs isentropic efficiency.

be found using the conservation of energy principle. Referring to Fig. 3, the power produced by the motor and the energy consumed by the pump and the compressor can be written as:

$$W_m = m_{113}\eta_{is}(h_1 - h_2), \tag{14}$$

$$W_c = m_{22}(h_8 - h_{15})/\eta_{is}, \tag{15}$$

$$W_p = m_{113}(h_5 - h_4), \tag{16}$$

where

W_m = Power generated by the hydraulic motor;
W_p = Energy consumed by the pump;
W_c = Energy consumed by the compressor.

The work required by the pump is very small compared to the energy consumed by the compressor; consequently, the isentropic efficiency of the pump is neglected to simplify the derivation. Applying the conservation of energy principle to the pump, the compressor, and the hydraulic motor, the following equation is obtained by combining equations (14), (15) and (16):

$$\frac{m_{22}}{m_{113}} = \frac{(h_1 - h_2)}{(h_8 - h_{15})}\eta_{is}^2 + \frac{(h_4 - h_5)}{(h_8 - h_{15})}\eta_{is}. \tag{17}$$

Since the cooling *COP* is defined as

$$COP = m_{22}(h_{14} - h_{13})/m_{113}(h_1 - h_7), \tag{18}$$

combining equations (17) and (18) results in the following equation:

$$COP = \frac{(h_1 - h_2)(h_{14} - h_{13})}{(h_1 - h_7)(h_8 - h_{15})}\eta_{is}^2 + \frac{(h_4 - h_5)(h_{14} - h_{13})}{(h_1 - h_7)(h_8 - h_{15})}\eta_{is}. \tag{19}$$

From Fig. 4, it can be seen that a decrease of isentropic efficiency from 1.0 to 0.9 causes an almost 20% drop in *COP*. This demonstrates the significant role of the motor and compressor isentropic efficiency in determining the system performance.

The next parametric analysis involves varying the R-22 and R-113 condenser operating temperature. The results are given in Figs 5, 6 and 7. In Fig. 5, cooling *COP* is plotted versus deviation of the condenser operating temperature from the base value listed in Table 1. It can be seen that *COP* suffers as the condenser's temperature is increased from the base value. This is due to the fact that a higher condenser operating temperature means a higher condenser operating pressure; consequently, more energy is required by the compressor to raise the fluid to that pressure.

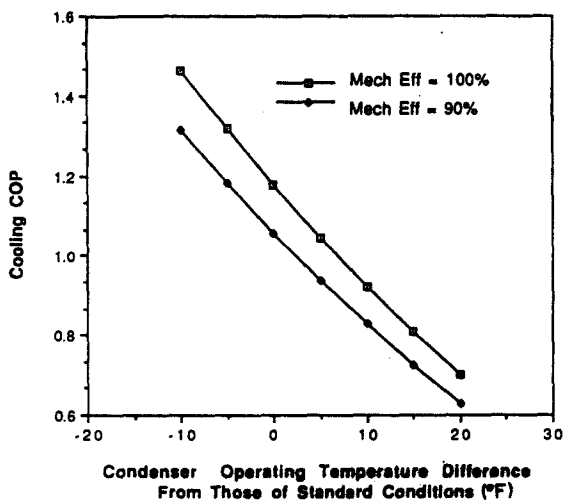

Fig. 5. Cooling *COP* vs condenser operating temperature.

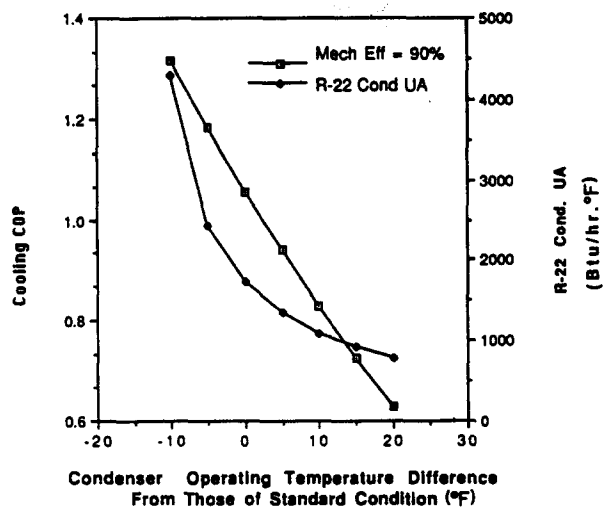

Fig. 6. Cooling *COP* and R-22 condenser *UA* vs condenser operating temperature.

As a result, the system *COP* will be lower since more energy needs to be supplied to the R-113 evaporator to operate the motor.

In addition to *COP*, the variation of the heat exchanger *UA* for the R-22 and R-113 condensers as a function of the condenser's operating temperature was also investigated. The results are presented in Figs 6 and 7 where cooling *COP* is plotted versus deviation of the operating temperature from the base value. As the condenser temperature increases, the R-22 condenser *UA* decreases. As a result, a smaller heat exchanger is enough to accommodate the system requirement.

The R-113 condenser *UA*, however, does not behave in the same manner as the R-22 condenser. The results indicate that as the condenser temperature is increased, the R-113 *UA* drops. Further increase of the condenser operating temperature will increase the R-113 *UA*, although the heat transfer process from the R-113 to the heat sink becomes easier.

This happens because increasing the R-113 condenser operating temperature beyond a certain limit shifts the cycle heat rejection process from the R-22 cycle to the R-113 cycle, i.e. more heat is released from the R-113 condenser than from the R-22 condenser. Consequently, even though the log mean temperature difference becomes larger, a larger heat exchanger is still required to accommodate this heat transfer.

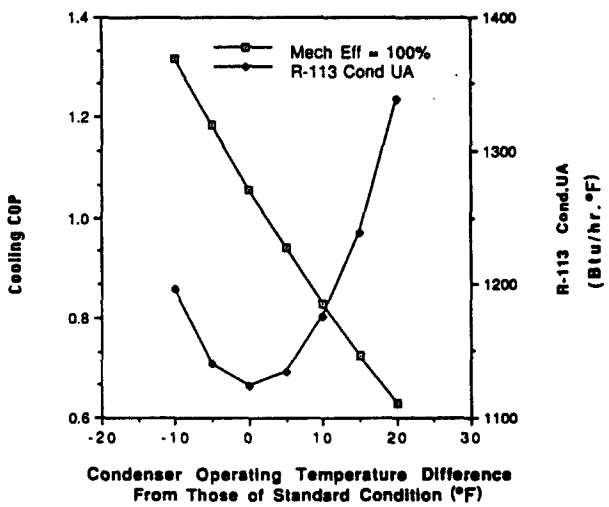

Fig. 7. Cooling *COP* and R-113 condenser *UA* vs condenser operating temperature.

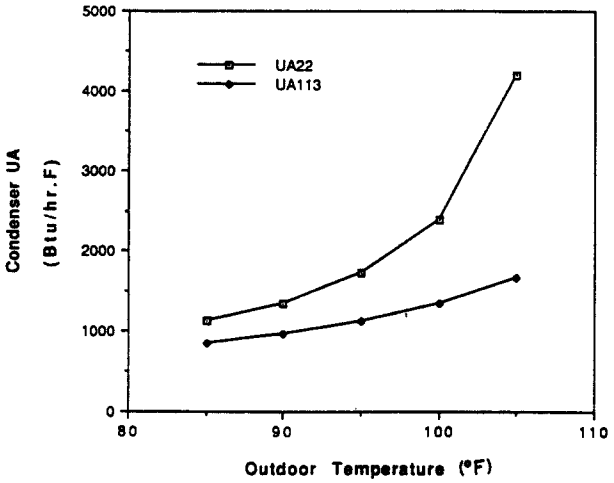

Fig. 8. Condenser *UA* vs outdoor temperature.

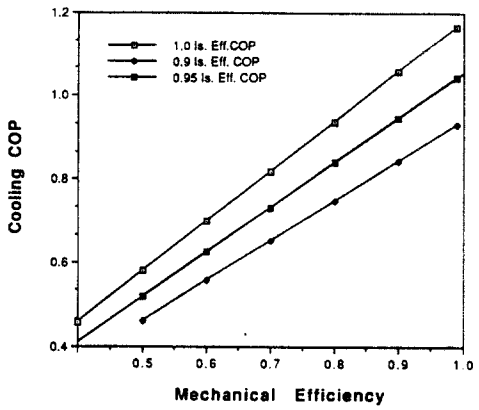

Fig. 9. Cooling *COP* vs mechanical efficiency.

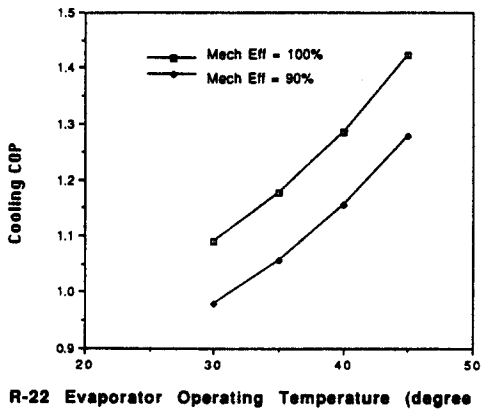

Fig. 10. Cooling *COP* vs R-22 evaporator temperature.

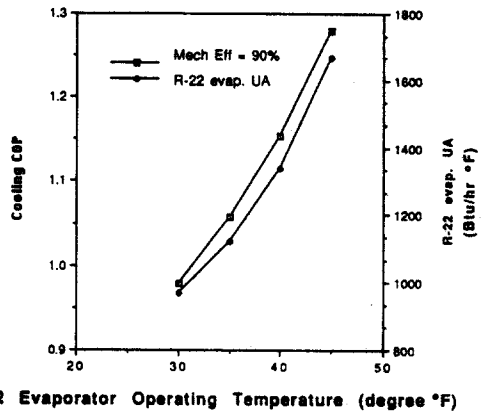

Fig. 11. Cooling *COP* and *UA* vs R-22 evaporator temperature.

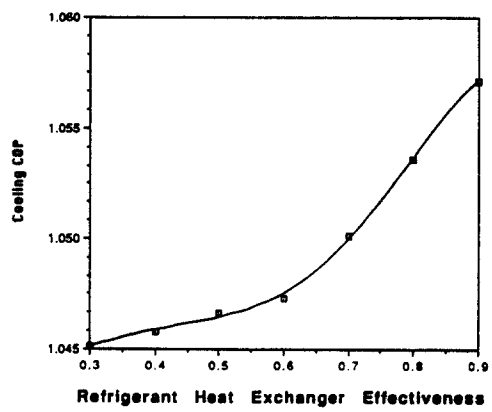

Fig. 12. Cooling *COP* vs refrigerant heat exchanger effectiveness.

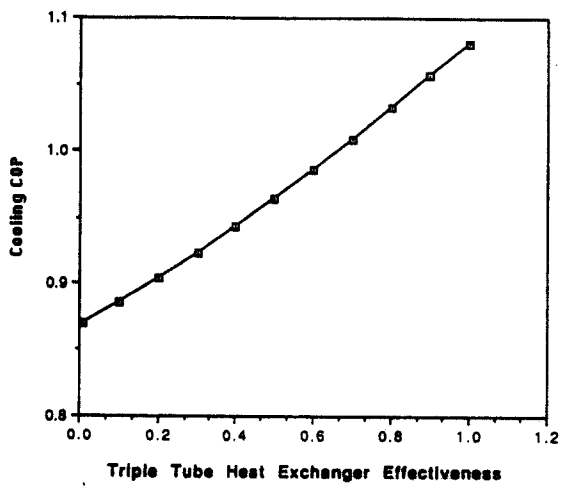

Fig. 13. Cooling *COP* vs triple tube heat exchanger effectiveness.

The next parameter to be analyzed is the outdoor or environmental temperature which affects only the condenser *UA*s. The result of this analysis is given in Fig. 8. It indicates that a higher outdoor temperature increases the condensers *UA* since the log mean temperature is decreased.

Figure 9 describes the *COP* variation with respect to the system mechanical efficiency. As expected, lower mechanical efficiency causes a lower *COP*. The energy loss due to the mechanical inefficiency occurs in the motor driving the pump and the compressor. It can also be observed in the figure that the effect of mechanical efficiency upon the system performance is not as significant as that of the isentropic efficiency. A 10% drop in mechanical efficiency results in about 10% drop in *COP* value, while a 10% reduction in isentropic efficiency causes an about 20% drop in the system performance.

Within the range given in Fig. 9, the relationship between cooling *COP* and the mechanical efficiency for 100% isentropic efficiency is given in equation (5) (a linear relationship). This equation is not valid as the mechanical efficiency approaches zero. At that point, the *COP* will be zero as well since the compressor and the pump will be idle.

In Fig. 10, the results of the variation of *COP* as the R-22 evaporator operating temperature is varied are presented. It is observed there that higher R-22 evaporator operating temperature increases the *COP*. However, it also increases the *UA* requirement for the R-22 evaporator as described in Fig. 11.

Increasing the R-22 evaporator temperature increases *COP* since less work is required by the compressor to drive the compressor. The increasing requirement of the R-22 evaporator is caused by the decrease in log mean temperature between the indoor temperature and the evaporator temperature.

The next independent variable investigated was the refrigerant heat exchanger effectiveness. The results of the analysis are given in Fig. 12 where it is observed that the reduction of refrigerant heat exchanger effectiveness reduces the system *COP* slightly. Reducing the effectiveness from 0.9 to 0.3 resulted in a reduction in the *COP* value by just a little bit over 0.01 (1%). Consequently, eliminating this component from the system will not hurt system performance. In an air conditioning system, the elimination of the refrigerant heat exchanger can be justified if slugging is not a problem in the compressor. Tests have shown that the unique rolling diaphragm compressor to be used in this system is not sensitive to slugging, therefore this heat exchanger can be eliminated.

The last variable to be studied in the cooling mode operation is the triple tube heat exchanger effectiveness. As shown in Fig. 13, the effectiveness of the triple tube heat exchanger has a significant impact on the system *COP* where reducing the effectiveness from 1.0 to 0.01 causes a 14% decrease in performance. The presence of this component in the system is essential to keep the *COP* high.

RESULTS OF HEATING MODE PARAMETRIC ANALYSIS

In this portion of the study, the heat pump performance in the heating mode was investigated as a function of six independent variables. In order to determine the necessity of the presence of the refrigerant and triple tube heat exchangers, the effectiveness of these heat exchangers was varied. There were four operating conditions. The variables investigated were:

(1) R-113 evaporator operating pressure;
(2) R-22 evaporator operating temperature;
(3) System mechanical efficiency;
(4) Condensers operating temperature;
(5) Regfrigerant heat exchanger effectiveness;
(6) Triple tube heat exchanger effectiveness.

The heat pump performance in the heating mode is evaluated with heat source temperatures of 45 and 17°F. Other conditions are as stated in Table 1. The analysis conducted in the heating mode followed a pattern similar to the one conducted in the cooling mode where *COP* and *UA* are the objects of study. The results obtained are presented in Figs 14–25. Since two heat source temperatures are used, two *COP* values are given in most of those figures. They are COP_{45} and

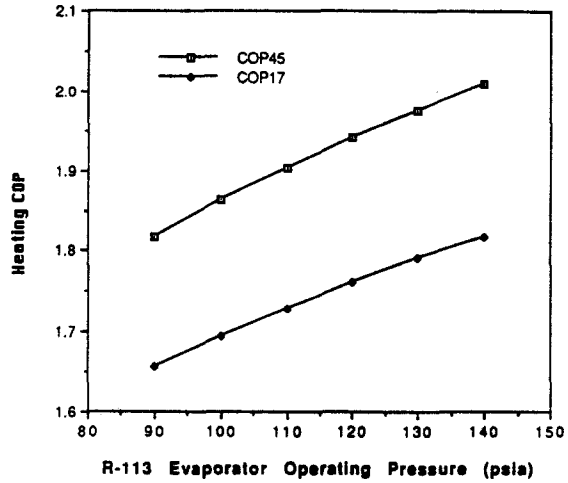

Fig. 14. Heating *COP* vs R-113 evaporator pressure.

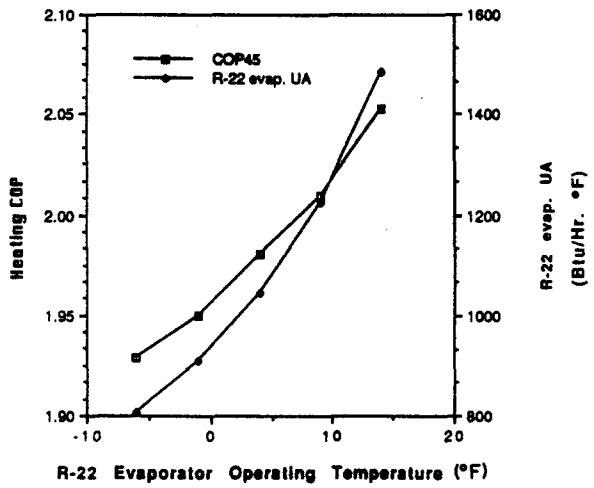

Fig. 15. *COP*45 and R-22 evaporator *UA* vs R-22 evaporator operating temperature

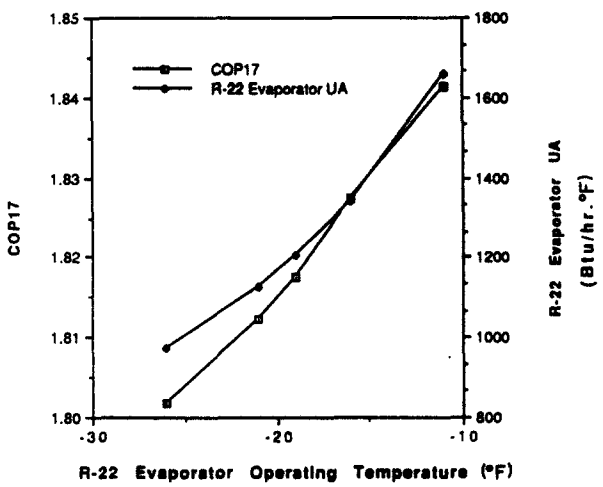

Fig. 16. *COP*17 and evaporator *UA* vs R-22 evaporator temperature.

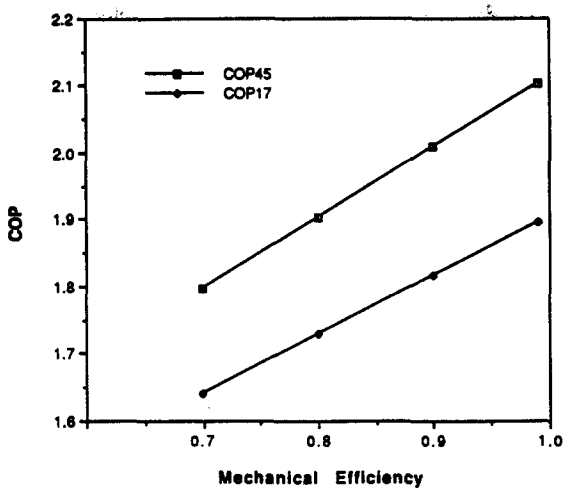

Fig. 17. Heating *COP* vs mechanical efficiency.

*COP*17 which corresponds to the *COP* values when the heat source temperature is 45 and 17°F, respectively.

Figure 14 describes the variation of *COP* as the R-113 evaporator operating pressure is varied. The results obtained show a similar trend with those obtained in the cooling mode where as the R-113 evaporator operating pressure is increased, the *COP* also increases. Therefore, it is better to operate the system in the heating mode at the highest R-113 evaporator pressure possible.

The next analysis involved investigating the effect of the R-22 evaporator operating temperature on the heating *COP*. The results of the analysis, given in Figs 15 and 16, show a similar trend with those obtained in the cooling mode operation. As the R-22 evaporator temperature is increased, the *COP* value increases as does the *UA*.

The *COP* increases since a higher R-22 evaporator temperature reduces the pressure differential across the compressor. As a result, less energy is required to drive the compressor. A higher evaporator temperature requires an increased *UA*, since the log mean temperature difference between the heat source (outdoor) and the R-22 becomes smaller. In order to maintain the amount of heat transfer to the R-22, a larger heat exchanger is required to perform the process.

As expected, a higher mechanical efficiency increases the *COP*. This result is given in Fig. 17, where the relationship between the *COP* and mechanical efficiency is linear. As observed in all these

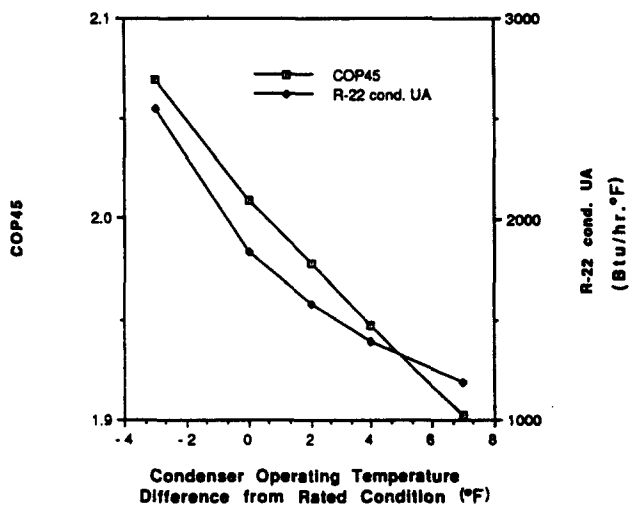

Fig. 18. *COP*45 and R-22 condenser *UA* vs condenser operating temperature.

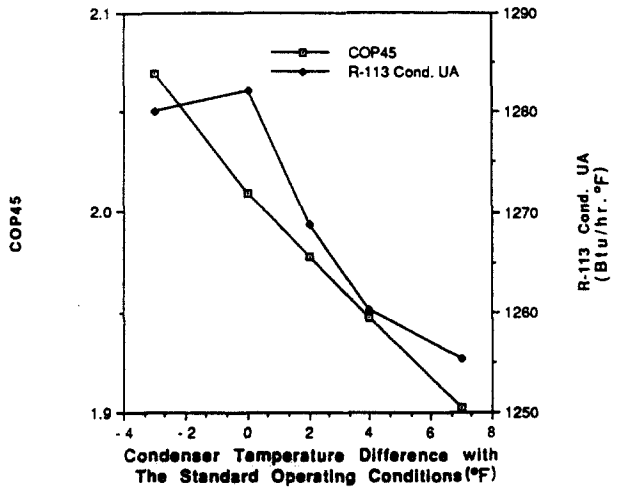

Fig. 19. *COP*45 and R-113 condenser *UA* vs condenser temperature.

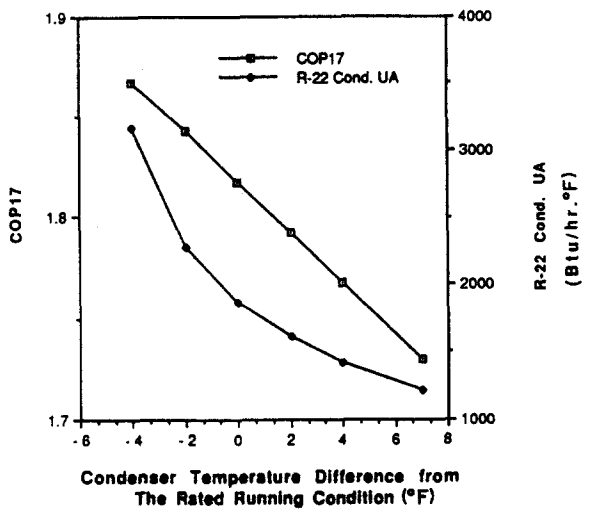

Fig. 20. *COP*17 and R-22 condenser *UA* vs condenser operating temperature.

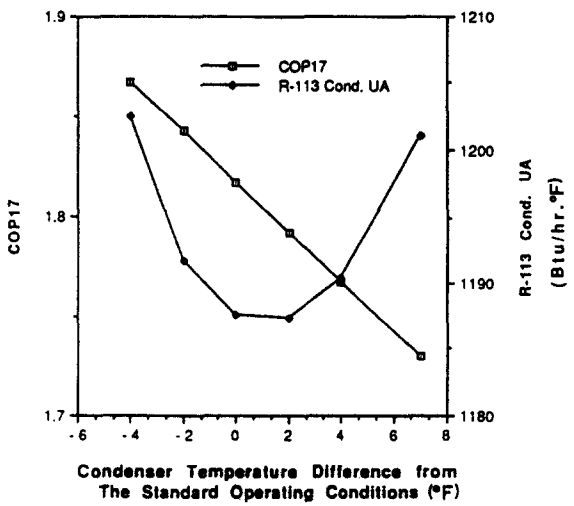

Fig. 21. *COP*17 and R-113 condenser *UA* vs condenser operating temperature.

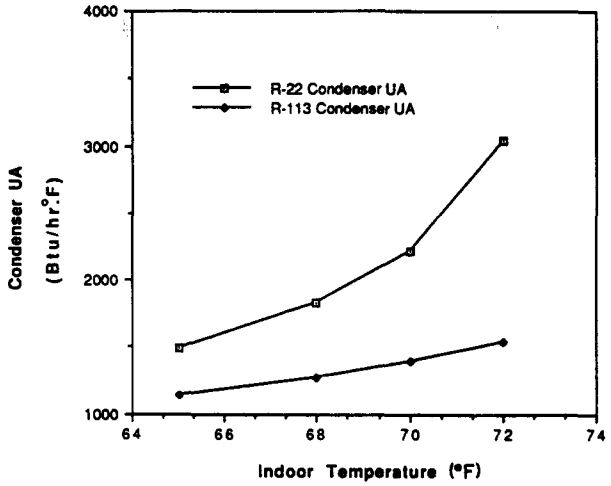

Fig. 22. Condenser *UA* vs indoor temperature for 45°F operation.

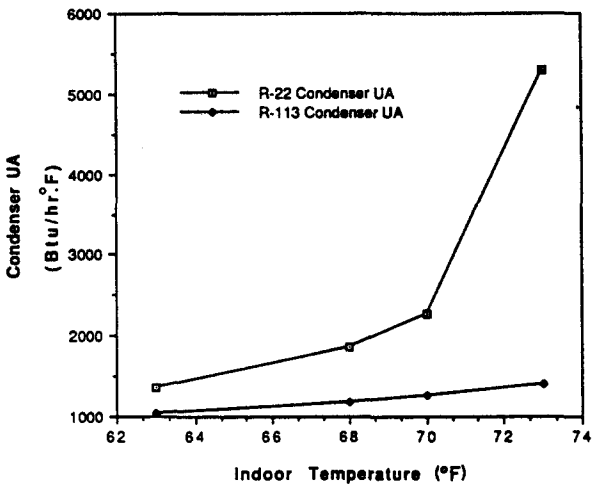

Fig. 23. Condenser *UA* vs indoor temperature for 17°F operation.

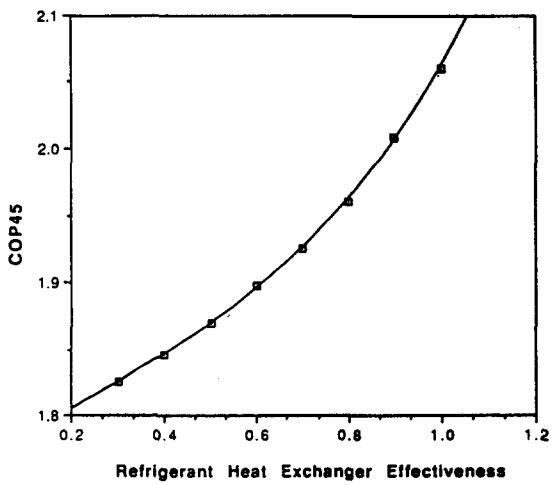

Fig. 24. Heating *COP* vs refrigerant heat exchanger effectiveness.

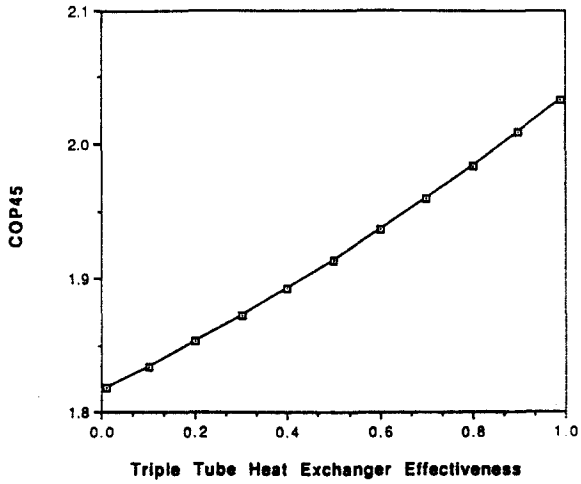

Fig. 25. Heating *COP* vs triple tube heat exchanger effectiveness.

figures, *COP*45 is always higher than *COP*17. This is due to the fact that at 45°F, the log mean temperature difference between the outdoor (heat source) and the evaporator temperature is larger than that at 17°F.

The next parameter investigated was the condenser operating temperature. The results are given in Figs 18–21. In all of those figures, the *COP* values, as well as the R-22 condenser *UA*, are observed to decrease as the condenser's operating temperature is increased. The reasons are the same as those given in the cooling mode operation.

In Figs 22 and 23, the variation of condenser *UA* with respect to the indoor temperature is further investigated. In this case, the condenser's operating temperature is fixed, and only the indoor temperature is varied. Consequently, only the heat exchangers *UA* values are affected, not the *COP*. As in the case of this cooling mode operation, the condenser's *UA*s increase as the indoor temperature is increased.

The refrigerant heat exchanger effectiveness is the next parameter investigated, in order to determine if the presence of this component in the heat pump system is justified. The result of the analysis is presented in Fig. 24, where it is observed that higher effectiveness increases the heating *COP* quite significantly. However, the heating *COP* of this heat pump system is quite high, more than 2.0 with 100% refrigerant heat exchanger effectiveness. Reducing the effectiveness by 80% resulted in slightly over 10% performance drop of this system. Since the *COP* is initially more than 2.0, elimination of this component from the system will decrease the *COP* to about 1.8, which is still acceptable in many applications.

The last parameter varied is the triple tube heat exchanger effectiveness. The results are given in Fig. 25. It is observed there that the elimination of this component from the system reduces the heating *COP* by about 0.2 (approximately 10% performance drop). Combined with the effect of this component on the cooling mode operation, the presence of the triple tube heat exchanger in the heat pump system is imperative to keep the *COP* high.

CONCLUSIONS

From the results of the analysis above, the following conclusions can be made:

(1) To obtain the highest *COP* possible, the operation conditions should be set at:
the highest possible R-113 evaporator operating pressure;
the highest possible R-22 evaporator operating pressure.

(2) The presence of the triple tube heat exchanger inside the system is essential; however, the presence of the refrigerant heat exchanger is optional depending on the cost. The function

Table 2. Comparison of proposed cycle with other cycles

	Brayton	Swenson's	Proposed cycle	Heat pump
Cooling *COP*	0.85	0.7	1.06	1.138
Heating *COP*	1.00	1.45	2.01	1.182

of the recuperative heat exchanger can be incorporated with the function of the triple tube heat exchanger.

The overall system performance is good in both heating and cooling mode. Table 2 presents *COP* at rated conditions for this system and the other systems mentioned earlier. Combined cooling and heating performance should make this cycle competitive.

REFERENCES

1. D. Friedman, Light commercial Brayton/Rankine space conditioning system, in *Proc. 12th Intersociety Energy Conversion Engineering Conference*, Washington, D.C., 28 Aug–2 Sept., p. 172 (1977).
2. P. F. Swenson and R. K. Rose, Development of a high seasonal performance factor gas heat pump, in *Proc. 12th Intersociety Energy Conversion Engineering Conference*, Washington, D.C., p. 390 (1977).